Proceedings of GT2007
ASME Turbo Expo 2007: Power for Land, Sea and Air
May 14-17, 2007, Montreal, Canada

GT2007-27048

SUBSYNCHRONOUS VIBRATIONS IN ROTATING MACHINERY – METHODOLOGIES TO IDENTIFY POTENTIAL INSTABILITY

Rahul Kar
Engineer,
Praxair Technology Center,
Tonawanda, New York.

John Vance
Professor, Mechanical Engineering,
Texas A&M University,
College Station, Texas.

ABSTRACT

Rotordynamic instability can be disastrous for the operation of high speed turbomachines in the industry. Most 'instabilities' are due to de-stabilizing cross coupled forces from variable fluid dynamic pressure around a rotor component, acting in the direction of forward whirl and causing subsynchronous orbiting of the rotor. However, all subsynchronous whirling are not unstable and methods to diagnose the potentially unstable kind from the benign are critical to the health of the rotor-bearing system.

In this study, methods to demarcate between the two are detailed. Orbit shape, "frequency tracking" and agreement of subsynchronous frequencies with known eigenvalues are used as diagnostic tools. It is shown that a change in synchronous phase angle produced by de-stabilizing cross coupled forces can be used as a definitive indicator of incipient instability. Typical signatures of subharmonic vibrations induced from non-linear stiffness of the rotor- bearing system are examined analytically and through experiments.

INTRODUCTION

A serious problem affecting the reliability of modern day high speed turbomachinery is "rotordynamic instability" evidenced as subsynchronous whirl. The cause of instability is never unbalance in a rotor bearing system. The de-stabilizing cross-coupled follower forces usually come from fluid pressure around the periphery of some rotor component, or from internal damping in the rotor assembly. In mathematical terms, "instability" is when the motion tends to increase without limit leading to destructive consequences. In most real cases, a "limit cycle" is reached, because the system parameters (stiffness/damping) do not remain linear with increasing amplitude. The rotor may then be operated at non-destructive amplitudes for years but needs rigorous monitoring tools, since any change in system parameters can destabilize the system and produce a rapid growth in amplitude. In the industry, large subsynchronous amplitudes are not a common occurrence, but are more destructive and difficult to remedy than imbalance problems when they do occur. Quite often, they are load or speed dependant, and build up to catastrophic levels under certain conditions. It is therefore of critical importance to study benign and potentially unstable subsynchronous vibrations and find ways of differentiating between the two.

Vibration signatures typical to instabilities were studied at length using several test rigs. A rig where a forward acting de-stabilizing air swirl around the rotor could be turned on and off (a large subsynchronous vibration was induced at the first eigenvalue above the first critical speed) was especially useful. Orbits from a potentially unstable whirl and a benign whirl were compared.

It was also discovered that the synchronous phase angle (the angle by which the unbalance vector leads the vibration vector) was affected by destabilizing cross coupled forces. The change in phase angle from cross-coupling can be a tool for the diagnostics of subsynchronous vibrations in the industry.

Subsynchronous rotor whirl from non-linear bearing supports is of particular interest, especially to explain the often noted fact that the onset of most asynchronous whirl phenomenon is at twice the induced whirl speed. The method of investigation is based upon a paper by F.F Ehrich [1],

claiming through analog computer simulations, that a planar vibrating system with non-linear stiffness would have a large subharmonic response at its first natural frequency when excited at twice its natural frequency. A numerical rotordynamic model of a short rigid rotor undergoing intermittent contact with the bearing housing was developed so that its stiffness varied as a step function of the displacement along the direction of contact. The system was excited by unbalance. Simulation results were verified with empirical data from a test rig where the non-linearity in bearing stiffness was artificially introduced.

DIAGNOSTIC INDICATORS OF FREQUENCIES

Several diagnostic indicators of subsynchronous frequencies were investigated and are discussed below:

Frequency tracking

If the subsynchronous frequency tracks the running speed at a fixed fraction of the synchronous, then it cannot be rotordynamic instability. If the machine speed cannot be varied then tracking is difficult to determine. An exception to this rule has been observed in a pump where the instability tracks the synchronous frequency at a constant fraction of 0.88[2]

Agreement of subsynchronous frequency with known eigenvalues of the system

Rotordynamic instability occurs at the damped natural frequency of the rotor-bearing system. The frequency can often be determined from an accurate rotordynamic model or from bump tests if the bearings are rolling-element.

Presence of higher harmonics or multiple frequencies

Subsynchronous frequencies caused by loose bearing clearances, loose bearing caps, or loose foundations may be excited by intermittent impact as the separated surfaces come together repeatedly as the machine runs. These impacts will excite a number of natural frequencies, none of which are unstable. Spectral analysis of the complex signal may expose a rich spectrum.

Orbit Shape – Ellipticity

De-stabilizing follower forces, modeled by cross-coupled stiffness, are always normal to the instantaneous rotor deflection vector (orbit radius). As Figure 1 shows, the follower force will be collinear with the velocity only if the orbit is circular. The force normal to the orbit radius becomes more oblique to the orbital velocity as the orbit becomes more elliptical. The rate of energy input to the orbit from the cross coupled force is given as,

$$J = \vec{F}_{cc}.\vec{v}$$

$$J = F_{cc} v \cos\theta$$

where, θ is the angle between the force and velocity vectors. b

Since, $\cos\theta \le 1, J_{\max} = F_{cc} v$ for $\theta = 0$ i.e. for a circular orbit.

Even though the orbit shape is not an absolute indicator of potential instability, it can be stated that highly elliptical orbits

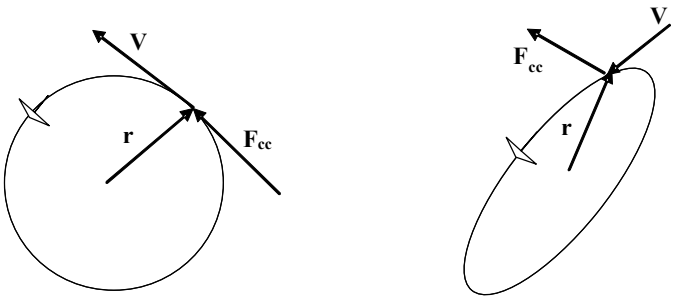

Figure 1: Follower forces

(almost a straight line) cannot become unstable from cross-coupled stiffness. For experimental determination, the orbit has to be filtered at the exact subsynchronous frequency.

Figure 2 and Figure 3 show filtered subsynchronous orbits from two different test rigs. The first is from a test rig which goes violently unstable due to internal friction at the interference fits.

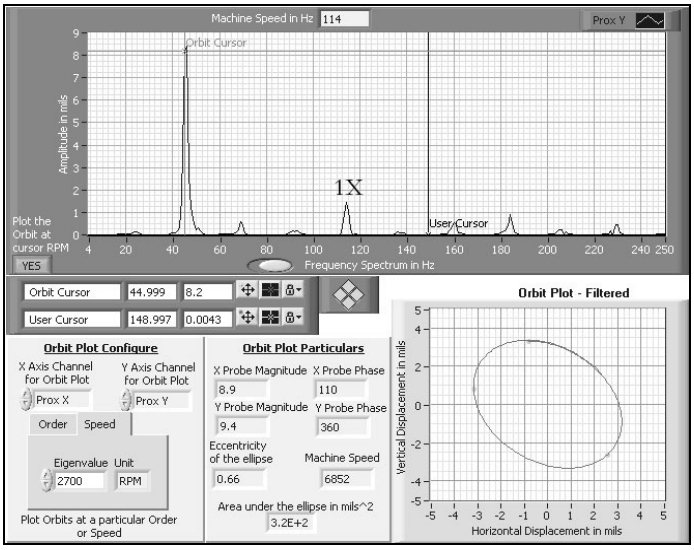

Figure 2: Instability from internal rotor friction

The second is benign vibration from a rotor kit with a worn out 'Oilite' bushing. Noticeably, the benign orbit from the latter case is highly elliptic.

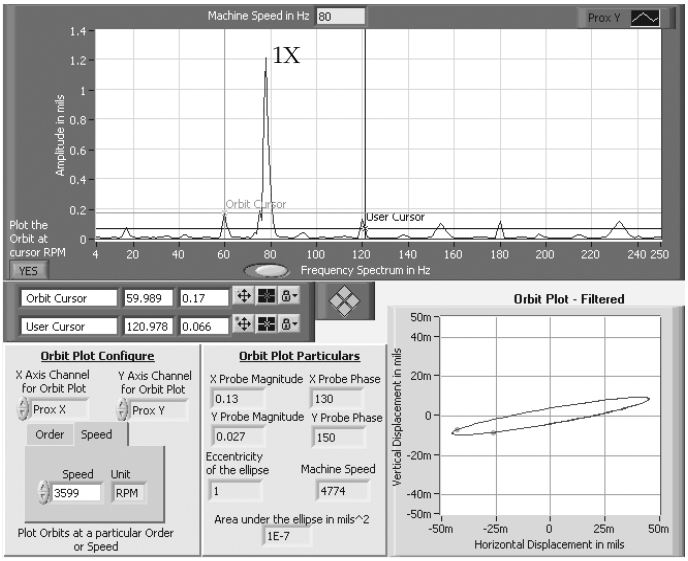

Figure 3: Benign subsynchronous vibration

SHORT RIGID ROTOR MODEL WITH NON-LINEAR BEARING STIFFNESS

The model illustrated in Figure 4 is used to simulate non-linear rotor-bearing stiffness due to intermittent contact of the rotor along the X-axis. For simplicity, the bearing stiffness is assumed to be isotropic. The bearing stiffness is much greater than the rotor stiffness so that there is practically no displacement of the surface during contact. The frame of reference is fixed and the generalized coordinates are X, Y and α.

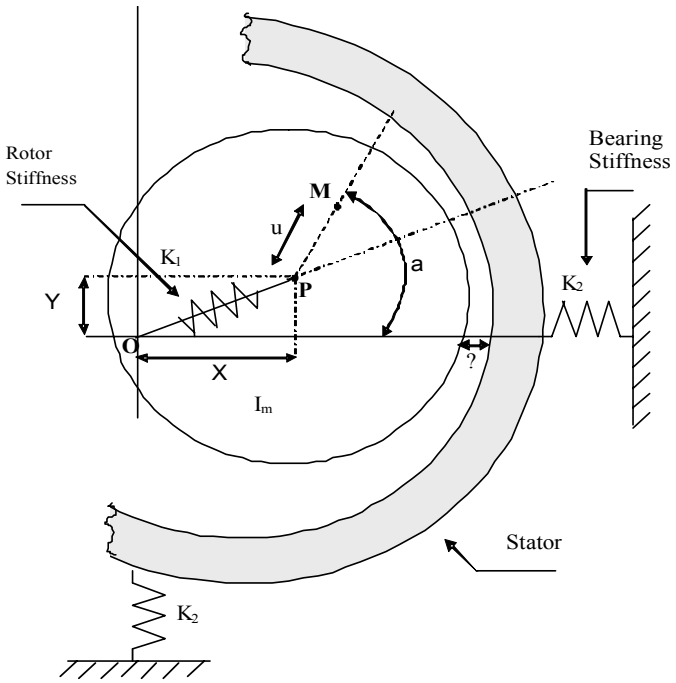

Figure 4: Nonlinear bearing stiffness model

Figure 5 shows the coordinates of the rotor used to develop the equations of motion to apply Newton's laws:

$\sum F_x = m\ddot{X}, \sum F_y = m\ddot{Y}, \sum \Gamma = I_m\ddot{\alpha}$, where,

F_x = restorative stiffness force (S_x) and 'damping force' (D_x) along the X-axis;
F_y = restorative stiffness force (S_y) and 'damping force' (D_y) along the Y-axis;
Γ = moments taken about point M;
Therefore,

$$\begin{aligned} m\ddot{X} + K_x X + C\dot{X} &= mu\ddot{\alpha}\sin\alpha + m\dot{\alpha}^2 u\cos\alpha \\ m\ddot{Y} + K_y Y + C\dot{Y} &= -mu\ddot{\alpha}\cos\alpha + m\dot{\alpha}^2 u\sin\alpha \\ I_m\ddot{\alpha} + K_x X(u\sin\alpha) + C\dot{X}(u\sin\alpha) - K_y Y(u\cos\alpha) - C\dot{Y}(u\cos\alpha) &= 0 \end{aligned} \quad (1)$$

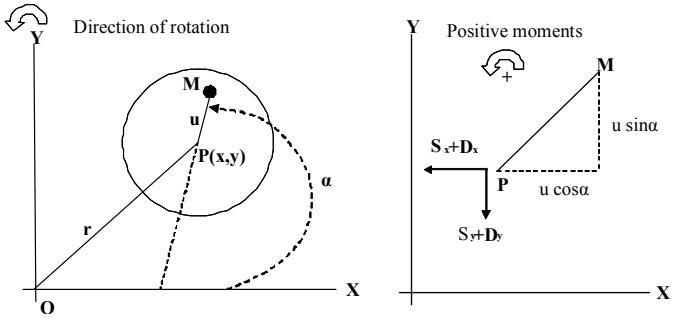

Figure 5: Model coordinates

For the model under consideration where the static stiffness of the system changes as a step function of the clearance (Δ), the system of equations (Equations (1)) can be divided into two cases:
Case 1: $X < \Delta$

$K_x = K_y = K_1$

$$\begin{aligned} m\ddot{X} + K_1 X + C\dot{X} &= mu\ddot{\alpha}\sin\alpha + m\dot{\alpha}^2 u\cos\alpha \\ m\ddot{Y} + K_1 Y + C\dot{Y} &= -mu\ddot{\alpha}\cos\alpha + m\dot{\alpha}^2 u\sin\alpha \\ I_m\ddot{\alpha} + K_1 X(u\sin\alpha) + C\dot{X}(u\sin\alpha) - K_1 Y(u\cos\alpha) - C\dot{Y}(u\cos\alpha) &= 0 \end{aligned} \quad (2)$$

Case 2: $X \geq \Delta$

$K_x = K_1 + K_2$, $K_y = K_1$

$$\begin{aligned} m\ddot{X} + (K_1 + K_2)X + C\dot{X} &= mu\ddot{\alpha}\sin\alpha + m\dot{\alpha}^2 u\cos\alpha \\ m\ddot{Y} + K_1 Y + C\dot{Y} &= -mu\ddot{\alpha}\cos\alpha + m\dot{\alpha}^2 u\sin\alpha \\ I_m\ddot{\alpha} + (K_1 + K_2)X(u\sin\alpha) + C\dot{X}(u\sin\alpha) - K_1 Y(u\cos\alpha) - C\dot{Y}(u\cos\alpha) &= 0 \end{aligned} \quad (3)$$

Define dimensionless spatial coordinates and time as -

$$x = \frac{X}{u}, y = \frac{Y}{u}, \tau = \omega_1 t, g = \frac{G}{u}, \delta = \frac{\Delta}{u}, \beta = \frac{K_1}{K_2},$$

where, G = radius of gyration, u = unbalance , $\omega_1 = \sqrt{K_1 / m}$ and $\xi = \frac{C}{2\sqrt{K_1 m}}$

Non-dimensional forms of Equation (2) and (3) are -
Case 1:

$$\begin{aligned} &\ddot{x} + 2\xi\dot{x} + x = \dot{\alpha}^2 \cos\alpha + \ddot{\alpha}\sin\alpha \\ &\ddot{y} + 2\xi\dot{y} + y = \dot{\alpha}^2 \sin\alpha - \ddot{\alpha}\cos\alpha \\ &\ddot{\alpha} + \frac{x}{g^2}\sin\alpha - \frac{y}{g^2}\cos\alpha + \frac{2\xi}{g^2}\dot{x}\sin\alpha - \frac{2\xi}{g^2}\dot{y}\cos\alpha = 0 \end{aligned} \quad (4)$$

Case 2:

$$\begin{aligned} &\ddot{x} + 2\xi\dot{x} + x\left(1 + \frac{1}{\beta}\right) = \dot{\alpha}^2 \cos\alpha + \ddot{\alpha}\sin\alpha \\ &\ddot{y} + 2\xi\dot{y} + y = \dot{\alpha}^2 \sin\alpha - \ddot{\alpha}\cos\alpha \\ &\ddot{\alpha} + \frac{x}{g^2}\left(1 + \frac{1}{\beta}\right)\sin\alpha - \frac{y}{g^2}\cos\alpha + \frac{2\xi}{g^2}\dot{x}\sin\alpha - \frac{2\xi}{g^2}\dot{y}\cos\alpha = 0 \end{aligned} \quad (5)$$

Equations (4) and (5) are integrated using Euler's method to obtain the response of the system to unbalance excitation in the time domain. The Fast Fourier Transform is used to convert the response to the frequency domain. Figure 6 shows the frequency response (predominantly 1X) at different rotational speeds (below twice the critical frequency) along the X-direction.

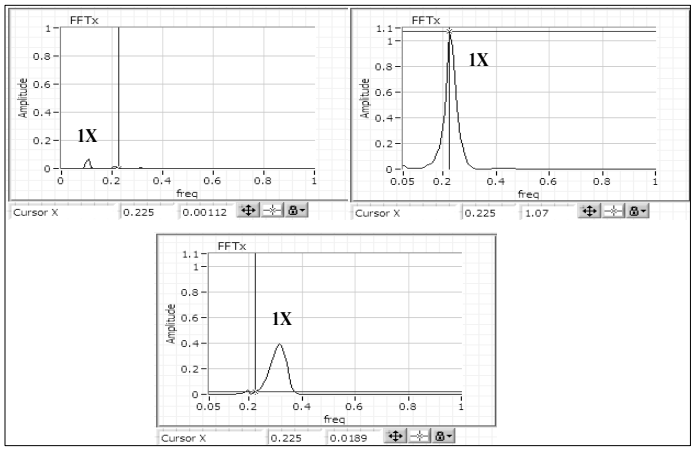

Figure 6: Spectrum with increasing speed

When the rotor speed is increased to twice the critical speed, a large subsynchronous component (0.5X) on the X-spectrum (Figure 7) is noted. The Y-response is largely synchronous. Note that the time trace resembles that shown by a typical unstable system. The orbit shows the expected inside loop. On increasing the speed (Figure 8), the subsynchronous vibration disappears which is atypical of instability.

Further proof that this phenomenon is due to non-linear stiffness was obtained from actual experiments conducted on a rig shown in Figure 9. The rotor is mounted on ball bearings constrained at the inner race (4) by a non-rotating cantilevered steel support rod (3).

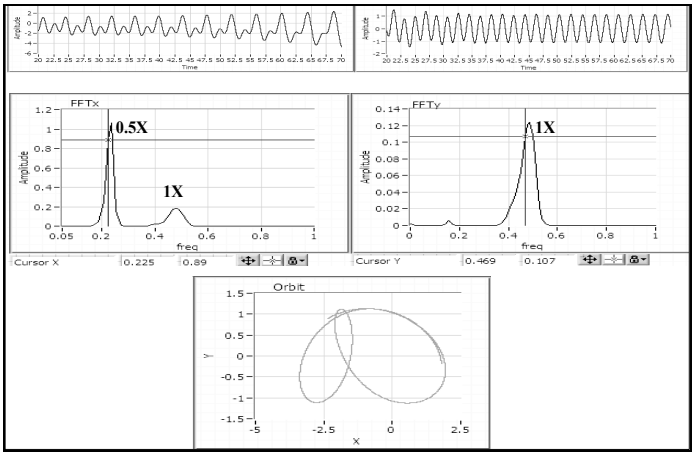

Figure 7: Spectrum and orbit at twice the critical speed

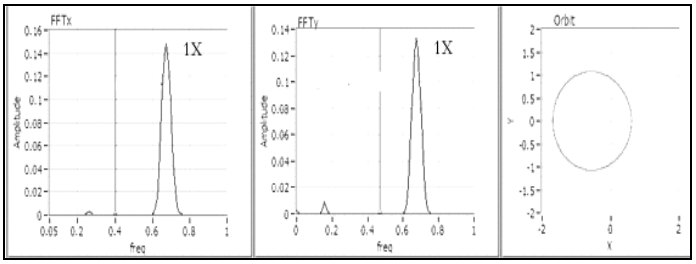

Figure 8: Spectrum at higher speeds

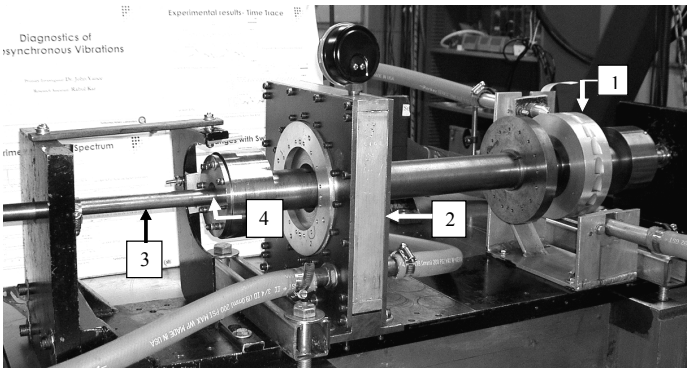

Figure 9: Test rig with swirl inducer

Pressurized air drives the air-turbine (1) up to a maximum speed of 7000 rpm. The swirl inducer housing (2) has nozzles arranged around the periphery of the rotor (Figure 10) to induce air swirl when pressurized. The air swirl is in the direction of rotor rotation and generates whirl instability from destabilizing cross coupled stiffness above the first critical speed (2100 rpm).

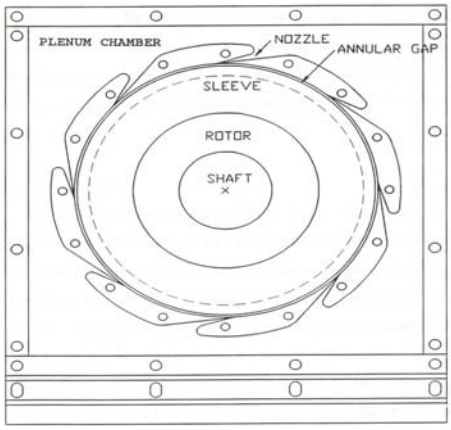

Figure 10: Swirl inducer

In order to introduce non-linearity in the bearing stiffness as a step function of the displacement along the horizontal axis, a stiffener was constructed and mounted as shown in Figure 11 and Figure 12. Two calibrated orthogonally mounted eddy current proximity probes (X and Y) were used to capture vibration data from the rotor. Another proximity probe was used to read tachometer pulses from a raised notch on the rotor surface.

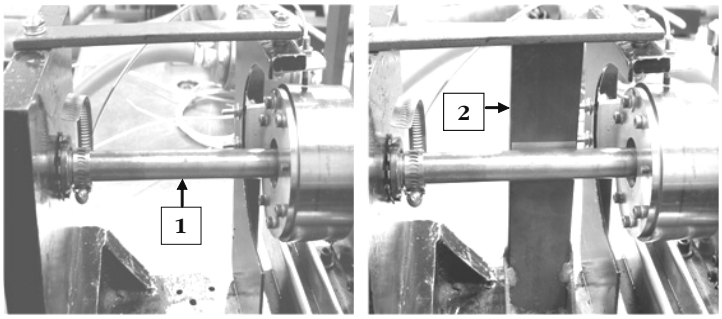

Figure 11: Cantilevered bearing support with nonlinear stiffener. 1: Cantilever, 2: Stiffener

F in lb	X in inches
0	0.00
5	0.00050
11	0.00110
15	0.00150
21	0.00210
26	0.00260
31	0.00310
41	0.00410
50	0.00500
70	0.00700
90	0.00900
100	0.01000

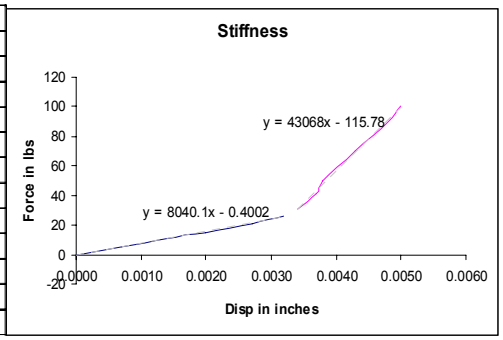

Figure 12: Stiffness measurements showing step nonlinearity

Spectral analysis of the probe signals normalized at the running speed show the occurrence of a large subharmonic response at twice the critical speed as shown in Figure 13. The waterfall plot obtained from run-up and coast-down of the rotor illustrates (Figure 14) that the subsynchronous vibration disappears on increasing the speed. Orbits (Figure 15) obtained using an analog oscilloscope also show similar behavior. The experiments are repeated for a linear system after removing the stiffener and no subharmonic response is noted. Snapshots of the spectrum at two different speeds are presented in Figure 16.

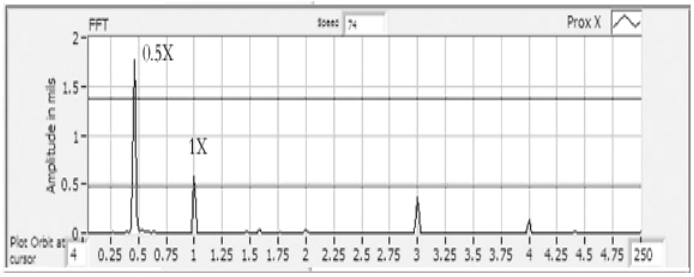

Figure 13: Order spectrum with nonlinear stiffness

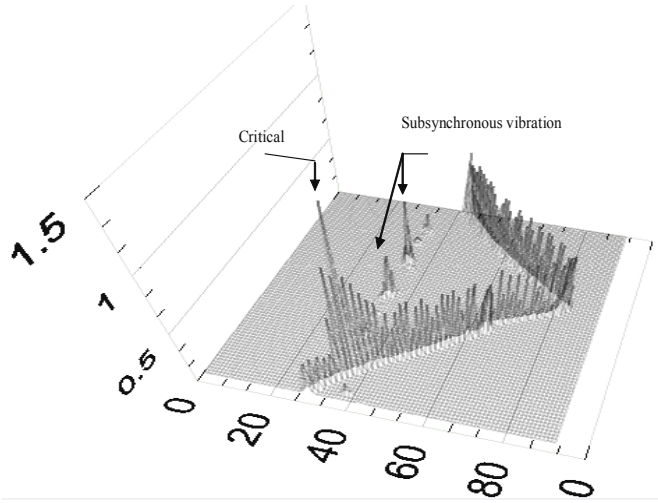

Figure 14: Waterfall with nonlinear stiffness

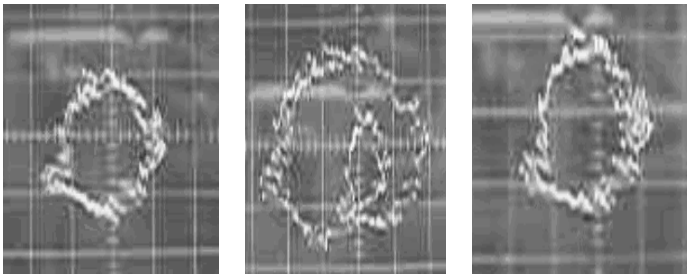

Figure 15: Orbits with nonlinear stiffness

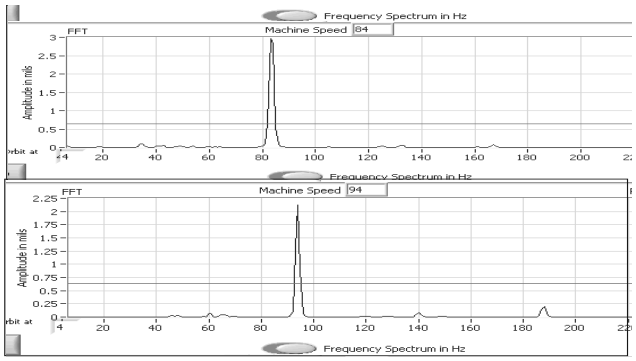

Figure 16: Spectrum with nonlinearity removed

DIAGNOSING SUBSYNCHRONOUS VIBRATIONS USING THE SYNCHRONOUS PHASE ANGLE

In rotordynamics, negative direct damping seldom occurs. Instead cross coupled stiffness, modeled as a follower force driving the forward going whirl orbit is usually the factor responsible for instability. The Jeffcott rotor model with cross coupled stiffness is a modal model for any real machine operating through its first critical speed. It may be represented mathematically as -

$$\begin{aligned} m\ddot{x} + c\dot{x} + Kx + k_{xy}y &= m\omega^2 u\cos\omega t \\ m\ddot{y} + c\dot{y} + Ky + k_{yx}x &= m\omega^2 u\sin\omega t \end{aligned} \tag{6}$$

where, K is the direct stiffness and k_{xy}, k_{yx} are cross coupled stiffness.

It is found that for the particular case where $k_{xy} = -k_{yx} = k$, $k > 0$; the cross coupled forces drive the rotor unstable in forward whirl (the common mode in real machines). It represents a type of force induced by fluid forces around a turbine, impeller, or fluid seal, or internal friction. The particular solution to Equation 6 is of interest. The amplitude and phase of synchronous vibration is given as –

$$\begin{aligned} |r| &= \sqrt{x^2 + y^2} = \frac{m\omega^2 u}{\sqrt{(K - m\omega^2)^2 + (\omega c - k)^2}} \\ \beta &= \tan^{-1}\left[\frac{\omega c - k}{K - m\omega^2}\right] \end{aligned} \tag{7}$$

In effect, the equivalent damping due to cross coupled stiffness becomes,

$$c_e = c - \frac{k}{\omega} \tag{8}$$

which is a function of the magnitude of cross coupled stiffness and the speed of rotation (ω).

Noticeably, the synchronous phase angle β is also affected by the cross coupled stiffness. It therefore can be a useful diagnostic value to determine whether the rotating system can have negative equivalent damping (instability)!

The synchronous phase angle is the angle by which the unbalance vector leads the vibration vector (Figure 17). The synchronous phase angle can be measured using the influence coefficient method [4], though actual measurement of the synchronous phase angle is not required. Instead it can be correlated to the phase displayed by industrial balancing machines using a simple relationship. Figure 18 is a setup for phase measurements to balance a rotor. All phase measurements are from the 'P' mark on the rotor which is the exact point below the X-probe, when the tachometer notch is lined up with the tachometer probe. $\bar{\theta}$ is the constant angular distance of the imbalance of the rotor from the 'P' mark. All angles are measured positive opposite to the direction of rotation. Following this convention,

$$\begin{aligned} \theta &= \bar{\theta} - \beta \\ \Delta\theta &= -\Delta\beta \end{aligned} \tag{9}$$

The rotor rig in Figure 9 was used for investigating the variation of β with cross coupled instability induced from a high pressure air swirl around the rotor..

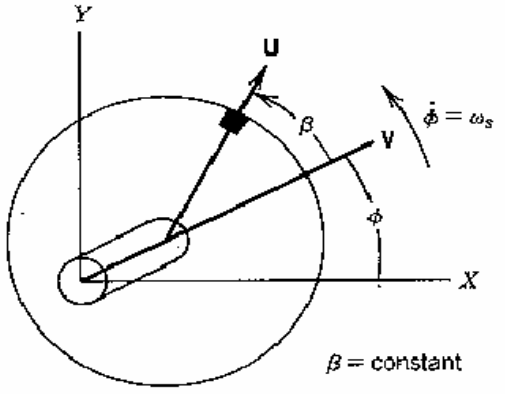

Figure 17: Phase angle β definition

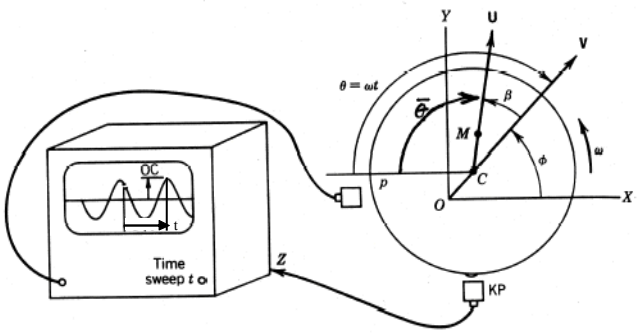

Figure 18: Phase angle θ from balancing instruments

Two sets of experiments were performed at 4200 rpm (twice the critical speed) – one with the swirl inducer turned on and one without. The frequency spectrum showed the presence of a strong subsynchronous component at the first eigenvalue in both the cases. In the first case (Figure 19), subsynchronous vibration was induced from non-linear bearing stiffness by

mounting a stiffener (as examined in Figure 11) and without air swirl around the rotor. The phase angle 'β' was almost 180 degrees, as is to be expected for a lightly damped rotor. In the second case (Figure 20) the swirl inducer was pressurized at 200 psi to induce de-stabilizing cross coupled forces (the stiffener was still mounted). The value of β changed to -174 degrees indicating the presence of a cross-coupled force. The instrument phase θ decreases from 91° to 82°. Thus, $\Delta\beta$ = -7.301 degrees and $\Delta\theta$ = 9.2 degrees.

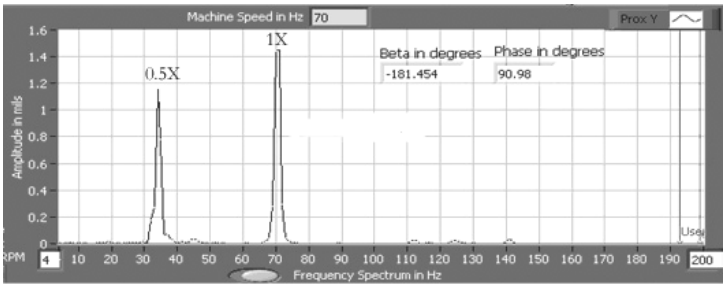

Figure 19: Phase with no cross coupling force from swirl

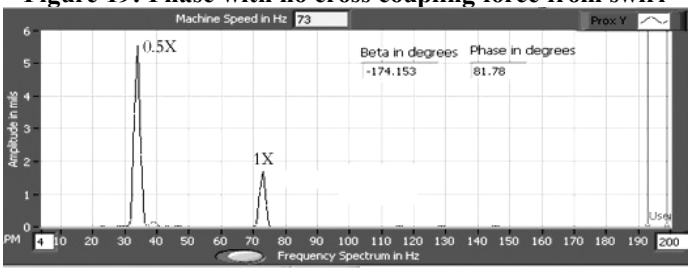

Figure 20: Phase with cross coupling force from swirl

The experiments were carried out at twice the critical speed to compare the phase changes from a benign and a potentially unstable subsynchronous vibration. Ideally, such diagnostic experiments should be carried out near the critical speed where the change of phase angle from cross coupling is more pronounced. However, the rotor in question had minimal direct damping and destabilizing cross coupling could have increased the critical response to dangerous proportions. Most industrial rotor-bearing systems have large direct damping and therefore can be tested near the critical speed. Further proof of diagnosing instability using the synchronous phase angle is illustrated in [4] with a rotordynamic model of the rig in Figure 9, by including and precluding bearings with cross coupled stiffness.

CONCLUSION

This research has studied methodologies to ascertain whether a subsynchronous vibration from a rotor is potentially unstable. It has examined vibration signatures typical to a rotating system with non-linear bearing or support stiffness, especially the large 0.5 X subharmonic response that is present when the rotor is running at twice its critical speed. The experimental results were substantiated with numerical simulations of a short rigid rotor with stiffness varying as a step function of the rotor displacement along a particular axis. The subsynchronous vibration in this case is benign, not a true instability.

A new method of diagnosing instabilities by observing changes in the synchronous phase angle was developed and verified with experiments.

Orbit shapes were demonstrated as a potential diagnostic tool (not absolute). Highly elliptical orbits are less likely to go unstable.

ACKNOWLEDGMENT

The authors wish to thank the Turbomachinery Research Consortium for funding the research. They are also grateful to Preston Johnson at National Instruments for assisting in developing LVTRC – the data acquisition software used for the above study.

REFERENCES

1. Ehrich, F.F., 1966, "Subharmonic Vibration of Rotors in Bearing Clearance", ASME-66-MD-1.
2. Valantas, R., Bolleter, U., 1998, "Solutions to Abrasive Wear-Related Rotordynamic Instability Problems in Prudhoe Bay Injections Pumps," Proceedings, Fifth International Pump Users Symposium, Texas A&M University.
3. Vance, J.M., 1988, *Rotordynamics of Turbomachinery*, John Wiley and Sons, New York.
4. Kar, Rahul, 2005, "Diagnostics of Subsynchronous Vibrations in Rotating Machinery – Methodologies to Identify Potential Instability", M.S. Thesis, Department of Mechanical Engineering, Texas A&M University, College Station.
5. Den Hartog, J.P., 1956, *Mechanical Vibrations*, 4th Edition, McGraw-Hill, New York.
6. Childs, D.W., 1981, "Fractional-Frequency Rotor Motion Due to Non-symmetric Clearance Effects", ASME- 81-GT-145.
7. Ferrara, P.L., 1977, "Vibrations in Very High Pressure Compressors", ASME-77-DET-15.
8. Wachel J.C., 1982, "Rotordynamic Instability Field Problems", Rotordynamic Instability Problems in High Performance Turbomachinery -1982, NASA Conference Publication 2250, Texas A&M University, College Station.